6th European Conference on Computational Mechanics (ECCM 6)
7th European Conference on Computational Fluid Dynamics (ECFD 7)
1115 June 2018, Glasgow, UK

MODIFICATION OF THE LEAST SQUARE MPS METHOD FOR THE HEAT CONDUCTION PROBLEMS

MASAYUKI TANAKA[1,2], RUI CARDOSO[1] AND HAMID BAHAI[1]

[1] Brunel University London
Kingston Lane, Uxbridge, London, UB8 3PH, United Kingdom
Masayuki.Tanaka@brunel.ac.uk

[2] Corporate Manufacturing Engineering Center, Toshiba Co., Ltd
33, Shinisogo-cho, Isogo-ku, Yokohama-shi, Kanagawa, 235-0017, Japan
masayuki11.tanaka@toshiba.co.jp

Key words: Least Square MPS method, Laser Irradiation, Multi-Resolution, Conservation

Abstract. In this work, new Least Square Moving Particle Semi-implicit (LSMPS) formulations for the modelling of the heat conduction in laser irradiation processes are developed. These new LSMPS formulations guarantee the conservation of the total thermal energy during the heat exchange between particles. By conducting the heat conduction simulations, in which the standard LSMPS method can provide accurate temperature distribution, and by comparing the results with an analytical solution, it was confirmed that the proposed method is as accurate as the standard LSMPS method. Moreover, the heat conduction with an external heat source, in which the total thermal energy is not conserved by using the standard LSMPS method, was successfully simulated by using the proposed method. The simulation of laser irradiation was also conducted and the validity of the proposed method has been confirmed by comparing numerical results with experimental data.

1 INTRODUCTION

Full Lagrangian particle methods have advantages when applied to simulations of multi-physics phenomena such as the free surface flow, fluid-structure interactions, multi-phase flow, phase change, etc. Particle methods such as the Moving Particle Semi-implicit method (MPS) [4] and Smoothed Particle Semi-implicit (SPH) [3] methods commonly calculate the derivatives by involving adjacent particles in a support domain utilising a weight function. However, the particle methods have been suffering from deterioration of the accuracy especially for boundary particles because their neighbouring particles are not distributed isotropically. This deterioration of the accuracy can take place not only for the boundary particles but also for any particles whose neighbouring particles are not distributed regularly. To overcome this inaccuracy, the Moving Least Square

(MLS) method has been applied to the MPS method, being labelled as the Least Square MPS (LSMPS) [6] method. The LSMPS method can use any polynomial degree for the interpolation of variables, and therefore it can provide more accurate results when compared with other particle based methods. More importantly, the LSMPS method can give accurate results even if the particles are distributed irregularly, which make them particularly suitable for accurate multi-resolution simulations [7].

The LSMPS method, however, does not guarantee the conservation of the physical quantities such as the momentum and energy. As Tanaka et al. [7] demonstrated, the momentum and kinematic energy are well conserved in some cases, however, the conservation of energy is not always fulfilled when least square techniques are used for heat conduction, such as for example for the laser irradiation process. The laser irradiation provides a large intake of thermal energy into the surface of the substrate. As a result, the surface of the substrate accounts for most of the higher temperature and therefore the temperature distribution is not smooth enough to be interpolated by the least square method. Therefore, the accurate interpolation is no longer possible even if the least square formulation is applied. Note that there are many formulations which can conserve the thermal energy in the traditional MPS and SPH methods [5], however, these methods are only accurate for regular particle distributions.

In this work, the LSMPS method is improved by considering the conservation of the total thermal energy so that the simulation of heat conduction for laser irradiation processes can be performed accurately. The multi-resolution particle arrangements are utilised for the efficient simulation by locating smaller particles only around the laser irradiation area. The accuracy of the proposed formulations is verified by comparing the results of multi-resolution simulations for the heat conduction with analytical solutions and experimental results.

2 STANDARD LSMPS METHOD

2.1 FORMULATION FOR DERIVATIVES

In the standard LSMPS method, the derivatives for an arbitrary scalar variable $f(\boldsymbol{x})$ at the location of particle i is formulated as follows:

$$\langle \boldsymbol{D}_{\boldsymbol{x}} f(\boldsymbol{x}) \rangle_i = \left\langle \boldsymbol{M}(\boldsymbol{x})^{-1} \right\rangle_i \langle \boldsymbol{m}(\boldsymbol{x}, f) \rangle_i \tag{1}$$

$$\langle \boldsymbol{M}(\boldsymbol{v}) \rangle_i = \sum_{j \neq i} \langle w \rangle_{ij} \boldsymbol{b}(\boldsymbol{v}_{ij}) \otimes \boldsymbol{b}(\boldsymbol{v}_{ij}) \tag{2}$$

$$\langle \boldsymbol{m}(\boldsymbol{v}, \phi) \rangle_i = \sum_{j \neq i} \langle w \rangle_{ij} \phi_{ij} \boldsymbol{b}(\boldsymbol{v}_{ij}) \tag{3}$$

where $\boldsymbol{x}$ is a coordinate, w is a weight function, $\boldsymbol{D}_{\boldsymbol{x}}$ is a set of differential operators, $\boldsymbol{M}$ is a moment matrix, $\boldsymbol{m}$ is a moment vector and $\boldsymbol{b}$ is a set of coordinates. Note that ϕ_i and $\langle \phi \rangle_i$ represent a value ϕ at the location of particle i, and $\langle \phi \rangle_{ij}$ denotes a value defined

between a pair of particles i and j. On the other hand, ϕ_{ij} is defined as a relative value between particles i and j, i.e., $\phi_{ij} = \phi_j - \phi_i$. For the second order interpolation in two dimensions, for example, $\boldsymbol{D_x}$ and $\boldsymbol{b}$ are given as follows:

$$\boldsymbol{D_x} = \left[\begin{array}{ccccc} \dfrac{\partial}{\partial x} & \dfrac{\partial}{\partial y} & \dfrac{\partial^2}{\partial x^2} & \dfrac{\partial^2}{\partial x \partial y} & \dfrac{\partial^2}{\partial y^2} \end{array} \right]^T \tag{4}$$

$$\boldsymbol{b}(\boldsymbol{v}) = \left[\begin{array}{ccccc} x & y & x^2 & xy & y^2 \end{array} \right]^T \tag{5}$$

The weight function w in the LSMPS method is normally defined as:

$$\langle w \rangle_{ij} = \begin{cases} \left(1 - \dfrac{|\boldsymbol{x}_{ij}|}{\langle R \rangle_{ij}}\right)^2 & \left(|\boldsymbol{x}_{ij}| \leq \langle R \rangle_{ij}\right) \\ 0 & \left(|\boldsymbol{x}_{ij}| > \langle R \rangle_{ij}\right) \end{cases} \tag{6}$$

where R is the radius of the support domain.

2.2 DISCRITISATION FOR HEAT CONDUCTION PROBLEMS

The governing equation for the heat conduction problem is defined and can be transformed as follows:

$$\int \frac{\partial(\rho h)}{\partial t} dV = \int \nabla \cdot (k \nabla T)\, dV = \int \left(k \nabla^2 T + \nabla k \cdot \nabla T\right) dV \tag{7}$$

Equation (7) can be discretised directly by utilising the LSMPS method.

2.3 MULTI-RESOLUTION MODELLING

The LSMPS method enables more accurate interpolations even when the size of the particles differs. However, when the diameters of the particles are varied, a one-way particle interaction might occur. To prevent this one-way particle interaction, the radius of the support domain for the multi-resolution simulation is defined between particles i and j as follows:

$$\langle R \rangle_{ij} = \frac{R_i + R_j}{2} \tag{8}$$

By defining the radius of the support domain like this, the one-way particle interaction is avoided. This feature is important for the conserving formulation described afterwards. Note that it is verified that the accuracy for the derivatives is good enough even if the radius of the support domain is changed as in Equation (8) [7].

3 PROPOSED METHOD

The improvements made for the LSMPS method for the thermal problem with laser irradiation are detailed in this section. In the proposed method, a surface integral is formulated based on the LSMPS method, and then the governing equation fo the heat conduction is discretised as heat fluxes between particles.

Let us start with the divergence theorem for an arbitrary vector field $\boldsymbol{v}$:

$$\int \nabla \cdot \boldsymbol{v} dV = \oint \boldsymbol{v} \cdot \boldsymbol{dS} \tag{9}$$

The left hand side of Equation (9) can be discretised by using the LSMPS method in the following way:

$$\int \nabla \cdot \boldsymbol{v} dV \approx V_i \left\langle \nabla \cdot \boldsymbol{v} \right\rangle_i = V_i \sum_{j \neq i} \boldsymbol{v}_{ij} \cdot \mathbf{G} \left(w_{ij} \boldsymbol{H}_i \left\langle \boldsymbol{M}^* \left(\boldsymbol{x} \right)^{-1} \right\rangle_i \boldsymbol{b} \left(\frac{\boldsymbol{x}_{ij}}{L_i} \right) \right) \tag{10}$$

where the operator $\boldsymbol{G}$ is an extraction for a gradient from a set of derivatives, e.g., $\boldsymbol{G}\left(\boldsymbol{D}_{\boldsymbol{x}}\right) = \left[\begin{array}{cc} \frac{\partial}{\partial x} & \frac{\partial}{\partial y} \end{array} \right]^T$. In order to obtain the surface integral from the discretisation for the LSMPS method, Equation (10) is transformed as follows:

$$\int \nabla \cdot \boldsymbol{v} dV \approx \sum_{j \neq i} \frac{\boldsymbol{v}_i + \boldsymbol{v}_j}{2} \cdot \left\langle \boldsymbol{S} \left(\boldsymbol{x} \right) \right\rangle_{ij} + \boldsymbol{v}_i \cdot \left\langle \boldsymbol{B} \left(\boldsymbol{x} \right) \right\rangle_i \tag{11}$$

where $\boldsymbol{S}$ and $\boldsymbol{B}$ are called the surface vector and the boundary vector respectively as defined below:

$$\left\langle \boldsymbol{S} \left(\boldsymbol{v} \right) \right\rangle_{ij} = \mathbf{G} \left(2 V_i \left\langle w \right\rangle_{ij} \left\langle \boldsymbol{M} \left(\boldsymbol{v} \right)^{-1} \right\rangle_i \boldsymbol{b} \left(\boldsymbol{v}_{ij} \right) \right) \tag{12}$$

$$\left\langle \boldsymbol{B} \left(\boldsymbol{v} \right) \right\rangle_i = -\mathbf{G} \left(2 V_i \left\langle \boldsymbol{M} \left(\boldsymbol{v} \right)^{-1} \right\rangle_i \sum_{j \neq i} \left\langle w \right\rangle_{ij} \boldsymbol{b} \left(\boldsymbol{v}_{ij} \right) \right) \tag{13}$$

Regarding that $\frac{\boldsymbol{v}_i + \boldsymbol{v}_j}{2}$ is the vector between particles i and j, i.e., $\left\langle \boldsymbol{v} \right\rangle_{ij} = \frac{\boldsymbol{v}_i + \boldsymbol{v}_j}{2}$, the surface integral can be formulated as follows:

$$\oint \boldsymbol{v} \cdot \boldsymbol{dS} \approx \sum_{j \neq i} \left\langle \boldsymbol{v} \right\rangle_{ij} \cdot \left\langle \boldsymbol{S} \left(\boldsymbol{x} \right) \right\rangle_{ij} + \boldsymbol{v}_i \cdot \left\langle \boldsymbol{B} \left(\boldsymbol{x} \right) \right\rangle_i \tag{14}$$

This equation is a new formulation for a surface integral with a particle method. This equation is consistent with the standard LSMPS method, which means that it is generally accurate but in some cases it does not guarantee the conservation of the thermal energy. Note that the boundary vector $\boldsymbol{B}$ is zero when the particles are distributed on a regular grid. In this case, the surface integral is formulated as below:

$$\oint \boldsymbol{v} \cdot \boldsymbol{dS} \approx \sum_{j \neq i} \left\langle \boldsymbol{v} \right\rangle_{ij} \cdot \left\langle \boldsymbol{S} \left(\boldsymbol{x} \right) \right\rangle_{ij} \tag{15}$$

The governing equation for thermal conduction can be expressed by using the following surface integral:

$$\int \frac{\partial (\rho h)}{\partial t} dV = \int \nabla \cdot (k \nabla T)\, dV = \oint k \nabla T \cdot \boldsymbol{dS} \tag{16}$$

The flux-based formulation from Equation (15) can be applied to the surface integral at the right hand side of Equation (16), resulting in the following discretised governing equation for heat conduction:

$$\rho_i V_i \frac{\Delta h_i}{\Delta t} = \sum_{j \neq i} \langle k \nabla T \rangle_{ij} \cdot \langle \boldsymbol{S}(\boldsymbol{x}) \rangle_{ij} \tag{17}$$

There are however some circumstances where Equation (17) does not conserve the total thermal energy due to the surface vector not being symmetric for a pair of particles i and j, i.e., $\langle \boldsymbol{S}(\boldsymbol{x}) \rangle_{ij} \neq -\langle \boldsymbol{S}(\boldsymbol{x}) \rangle_{ji}$. For the conservation of the total thermal energy, the surface vector between particles i and j must satisfy the equation below:

$$\langle \boldsymbol{S}(\boldsymbol{x}) \rangle_{ij} = -\langle \boldsymbol{S}(\boldsymbol{x}) \rangle_{ji} \tag{18}$$

Assuming Equation (18) is satisfied, Equation (17) is replaced with the following equation:

$$\rho_i V_i \frac{\Delta h_i}{\Delta t} = \sum_{j \neq i} \langle k \nabla T \rangle_{ij} \cdot \langle \boldsymbol{S}^*(\boldsymbol{x}) \rangle_{ij} \tag{19}$$

where,

$$\langle \boldsymbol{S}^*(\boldsymbol{v}) \rangle_{ij} = \frac{1}{2} \left(\langle \boldsymbol{S}(\boldsymbol{v}) \rangle_{ij} - \langle \boldsymbol{S}(\boldsymbol{v}) \rangle_{ji} \right) \tag{20}$$

There is another important condition required for the conservation of the total thermal energy which is the one related with the symmetry of the heat flux. If the heat flux $\langle k \nabla T \rangle_{ij}$ is symmetric for a pair of particles i and j, then Equation (19) guarantees the conservation of the thermal energy.

In this work, a few formulations for the heat flux $k \nabla T$ are proposed. Normally, the heat flux between particles i and j is expressed as:

$$\langle k \nabla T \rangle_{ij} = \frac{1}{2} \left(\langle k \nabla T \rangle_i + \langle k \nabla T \rangle_j \right) \tag{21}$$

This can be calculated by using the standard LSMPS method and this formulation is referred as the LSMPS-like flux. However, this formulation can lead to the overshooting or undershooting of enthalpies and temperatures. When using the traditional MPS method, the heat flux can be expressed as:

$$\langle k \nabla T \rangle_{ij} = \frac{k_i + k_j}{2} \frac{T_{ij}}{|\boldsymbol{x}_{ij}|} \frac{\boldsymbol{x}_{ij}}{|\boldsymbol{x}_{ij}|} \tag{22}$$

This formulation is referred as the MPS-like flux in this work. Although it lacks information in every direction other than the direction from particle i to particle j, it does not cause the referred overshooting or undershooting discussed above.

Table 1: List of methods used in this work

Label	Method	Heat Flux
LAP	Laplacian : Eq. (7)	-
FLX-L	the conserving flux method : Eq. (19)	the LSMPS-based flux : Eq. (21)
FLX-M	the conserving flux method : Eq. (19)	the MPS-based flux : Eq. (22)

4 SIMULATION RESULTS AND DISCUSSIONS

Several simulations were conducted by using the formulations proposed above. The methods with corresponding labelling for the simulations used in this work are listed in Table 1.

4.1 SIMULATION OF THE HEAT CONDUCTION PROBLEM WITH AN ANALYTICAL SOLUTION

In order to show that the proposed methods can be properly used for the transient heat conduction problem, the accuracy of the heat conduction simulation with each formulation was verified by comparing the simulated temperature distributions with an analytical solution. The following equation was used as the analytical solution for the transient heat conduction:

$$T(x,y,t) = \frac{\Delta T}{2}\left(\cos(\pi x) + \cos(\pi y)\right)\exp\left(-\frac{\pi^2 k t}{\rho c}\right) + T_0 + \Delta T \tag{23}$$

where T is the temperature, k is the thermal conductivity, ρ is the density, c is the specific heat and t is the time. Note that the physical properties are assumed to be constant throughout the simulations in this section and then Equation (23) satisfies the governing equation for the heat conduction from Equation (16).

The particles were located in the area of $0 \leq x \leq 1$ and $0 \leq y \leq 1$ and the symmetric boundary conditions were applied to the boundaries. Three particle arrangements shown in Figure 1 were used in this section: a regular particle arrangement with the diameter of 10 mm, an irregular particle arrangement with the diameter 10 mm and a multi-resolution particle arrangement. The irregular particle arrangement was created in the same manner as in the work by Tamai and Koshizuka [6], making the standard deviation to be 10% of the particles' diameter. The diameters of the smaller and larger particles in the multi-resolution particle arrangement were 10 mm and 5 mm respectively.

All methods listed in Table 1 were used for each geometry. The temperatures were evaluated on the line of x = 0.3. The density was 2700 kg/m^3, the thermal conductivity was 200 W/K·m and the specific heat was 900 J/kg·K.

The temperature distributions after simulating for 2500 sec are shown in Figure 2. For the regular particle arrangement, all methods were in good agreement with the analytical solution as shown in Figure 2(a). Figures 2(b) and 2(c) show that when the particles were not distributed regularly, the accuracy by the LSMPS-like flux method deteriorated. The

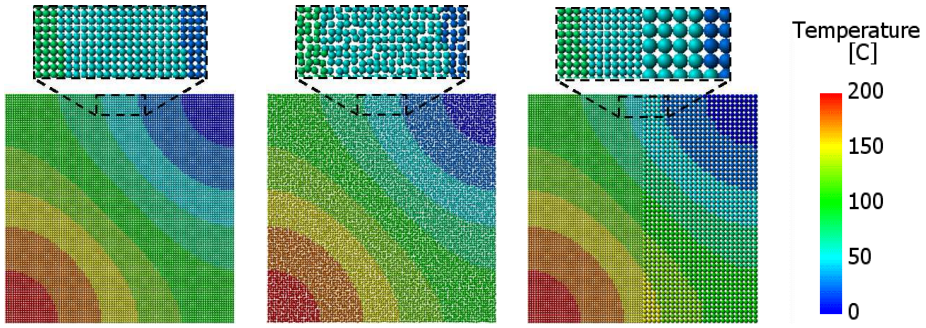

(a) Regular (b) Irregular (c) Multi-Resolution

Figure 1: Geometries for the heat conduction simulation with an analytical solution

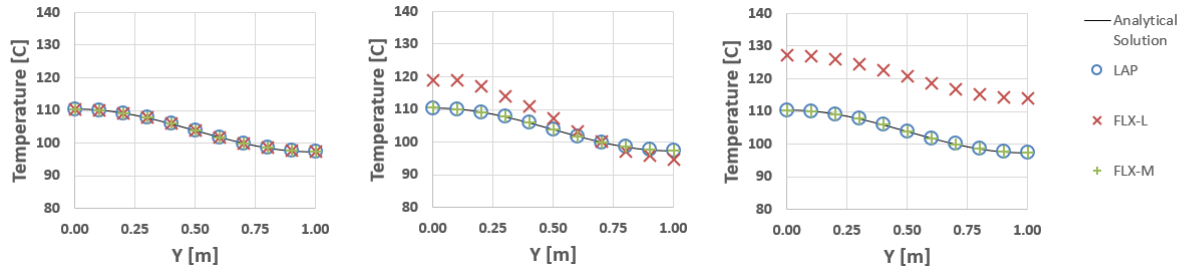

(a) Regular arrangement (b) Irregular arrangement (c) Multi-Resolution

Figure 2: Comparisons of the temperature distribution between the correct answer and the simulation results

reason for this deterioration of the accuracy is due to the LSMPS-like method resulting in the overshooting and undershooting as shown in the next section. Note that the standard LSMPS method (LAP) and the proposed method with the MPS-like flux (FLX-M) were both accurate for all cases in this section.

4.2 SIMULATION OF THE HEAT CONDUCTION PROBLEM WITH AN EXTERNAL HEAT SOURCE

In this section, heat conduction simulations considering an external heat source are demonstrated. The geometry used in the simulation was for a block with quadrangular cross-section, whose dimensions were 100 mm × 10 mm × 10 mm. A uniform heat flux was used as input for the quadrangular cross-section of the block and the heat was conducted along the length direction of the block. Four particle arrangements were used in the simulations as shown in Figure 3: two regular particle arrangements with the particles' diameter of 2.5 and 1.0 mm, an irregular particle arrangement with the diameter of 1.0 mm and a multi-resolution particle arrangement with the diameters ranging from 1.0 to 2.5 mm. All methods listed in Table 1 were used for each particle arrangement described just above.

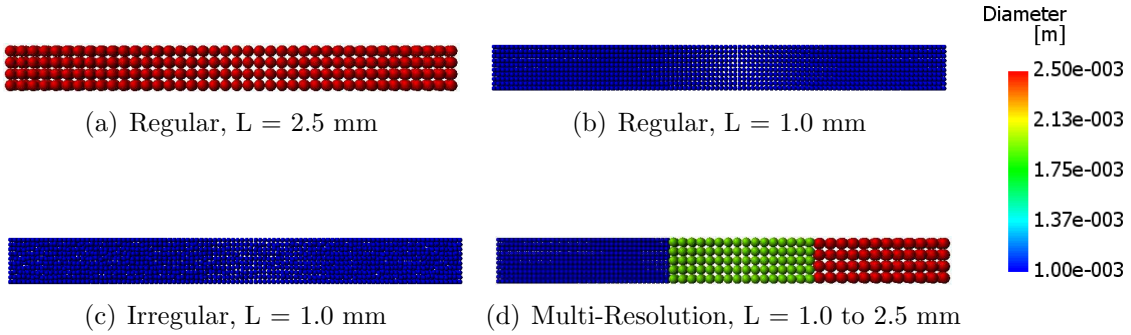

(a) Regular, L = 2.5 mm (b) Regular, L = 1.0 mm

(c) Irregular, L = 1.0 mm (d) Multi-Resolution, L = 1.0 to 2.5 mm

Figure 3: Geometries for the heat conduction simulations with the external heat source

The physical properties were the same as those used in section 4.1. The amount of heat flux used for the simulations was 10 W and the simulations were conducted for 100 sec time. The temperatures were monitored on the centre line of the block and along the length direction. The same simulation was conducted with ANSYS in order to be served as reference solution for comparison purposes.

The temperature distribution obtained for each particle arrangement by each method is shown in Figure 4. It is found that the standard LSMPS method, i.e. LAP, has large errors for almost all geometries. The temperatures obtained by LAP are higher than the results obtained by ANSYS for all measured points, which means that the total amount of the thermal energy is increased. This is mainly because the standard LSMPS method cannot calculate properly the heat flux from the external heat source. When a heat flux is given at a surface from an external heat source, only the surface particles have higher temperatures and the temperature distribution is no longer smooth enough to be interpolated by the least square method. This is why the LSMPS method has large errors for problems with external heat sources while it delivers accurate results for problems with smooth temperature distribution as the one from section 4.1.

The proposed methods, on the other hand, provided more accurate results for all geometries. This is because these methods guarantee the conservation of the thermal energy. Although the temperature distribution obtained by the LSMPS-like flux method (FLX-L) looks similar to the result provided by ANSYS from Figure 4, however, it gives the overshooting and undershooting, and then the temperature distribution is not smooth enough as shown in Figure 5. The temperatures plotted in Figure 4 were interpolated by the LSMPS method and the overshooting and undershooting were smoothed through the interpolation process. As a result, the temperature distribution looks smooth and accurate enough even though the actual temperature distribution is a bit far from the desired accurate results. On the other hand, Figure 5 shows that the distribution of the temperature provided by the MPS-like flux method is smooth enough for every particle arrangement.

4.3 SIMULATION OF THE LASER IRRADIATION

In this section, the simulations of the laser irradiation on a block were conducted and the dimensions of the melted region were compared with experimental results. The

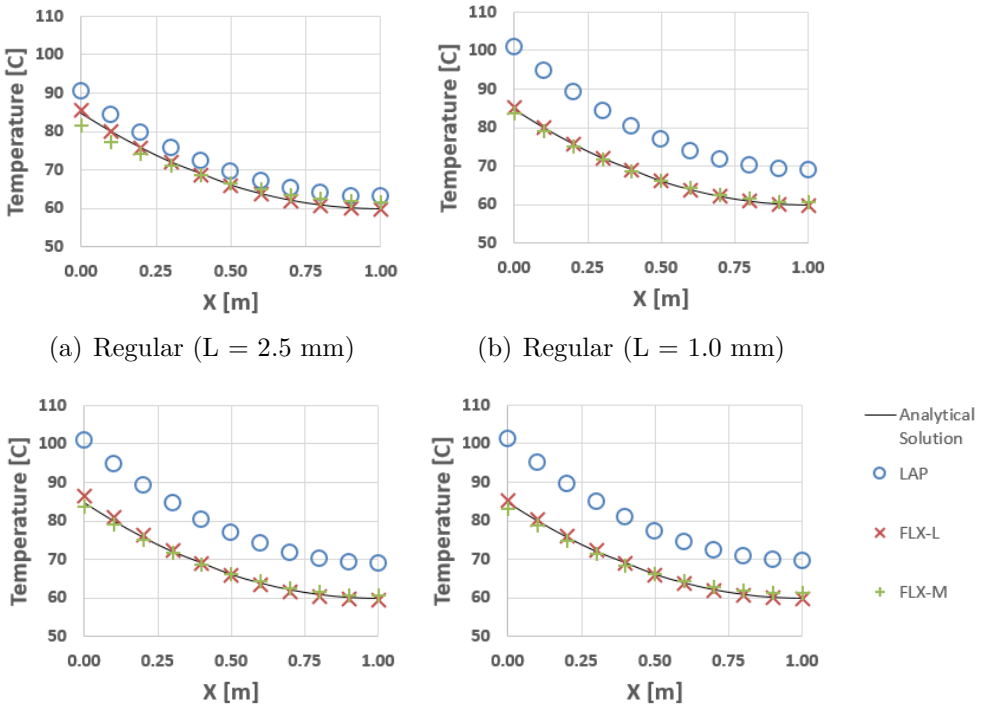

(a) Regular (L = 2.5 mm) (b) Regular (L = 1.0 mm)

(c) Irregular (d) Multi-resolution

Figure 4: Temperature profiles for the heat conduction simulation with the external heat source

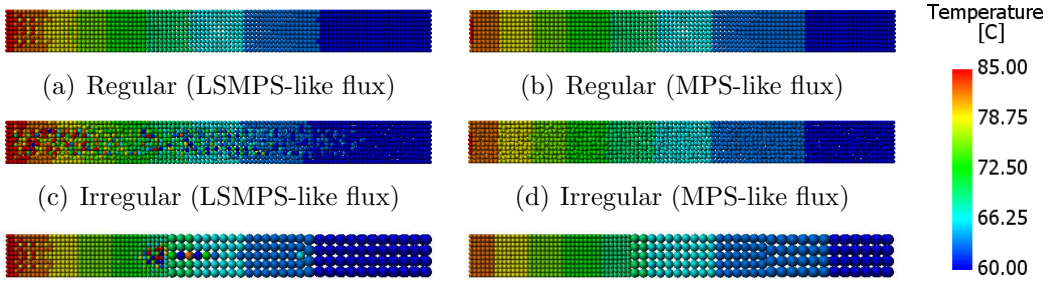

(a) Regular (LSMPS-like flux) (b) Regular (MPS-like flux)

(c) Irregular (LSMPS-like flux) (d) Irregular (MPS-like flux)

(e) Multi-resolution (LSMPS-like flux) (f) Multi-resolution (MPS-like flux)

Figure 5: Cross sections of the simulation results for the heat conduction simulation with the external heat source

Table 2: Laser conditions for the laser irradiation simulation

Laser Condition	Diameter mm	Power kW	Velocity m/s
A	1.04	0.33	2.08
B	1.44	0.68	4.17
C	2.04	1.36	8.33
D	2.87	2.68	16.67

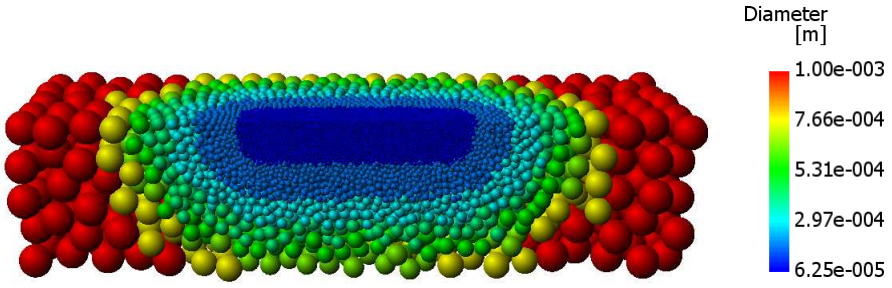

Figure 6: Geometry for the laser irradiation simulation

simulations demonstrated in this section are based on the experiments conducted by Ayoola et al. [1]. Four trial test cases were defined with different laser setups characterised by the spot diameter D, the laser power P and the velocity U. A summary of these test cases with corresponding laser parameters is described in Table 2, with the power density fixed to 41.5 kW/cm^2 and the total laser energy irradiated, during the period in which the laser moves by the same distance as the spot diameter, fixed to 160 J. The material for the block used in the experiments was the steel S275 and the physical properties used in the simulations were the same as the ones used in the work by Ayoola et al. [1]: the density was 7600 kg/m^3, the thermal conductivity was 42.636 W/m·K, the specific heat was 510 J/kg·K, the solidus temperature was 1490 °C, the liquidus temperature was 1500 °C and the heat of fusion was 2.5e+5 J/kg. The reflectivity was assumed to be 0.3. Note that there was no special treatment used for the particles whose temperature was above the liquidus temperature, and the fluid motion of the molten metal and the evaporation were not considered in this work.

The multi-resolution particle arrangement as shown in Figure 6 was utilised for the simulation. To calculate the heat transfer from the laser beam, the ray tracing algorithm e.g. [2] was applied. The laser beam was divided into as small areas as 0.1 mm and each area generated a ray with the thermal energy based on the Gaussian distribution of the laser power. Each simulation was conducted for the time corresponding to D/U. Note that it is assumed that the reflected laser beam does not interact with the specimen in this work. The MPS-like flux (FLX-M) was used for the flux formulation.

The spatial distributions for the maximum temperature, which is the highest temper-

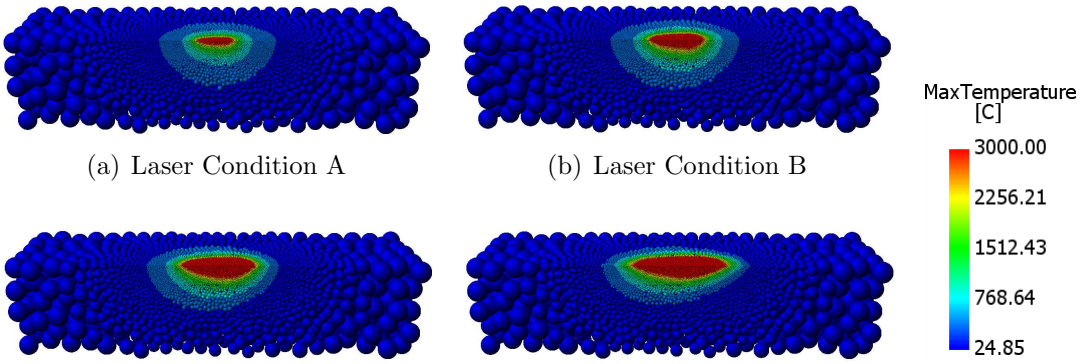

(a) Laser Condition A (b) Laser Condition B

(c) Laser Condition C (d) Laser Condition D

Figure 7: Maximum temperatures for the laser irradiation simulation

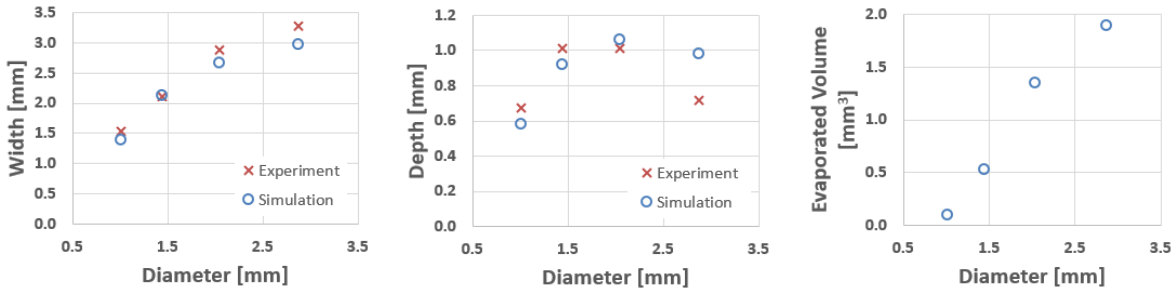

(a) Width (b) Depth (c) Evaporated Volume

Figure 8: Simulation results for the laser irradiation simulation

ature throughout the simulation for each particle, are illustrated in Figure 7. The region where the maximum temperature is higher than the liquidus temperature corresponds to the melted area. The widths and depths of the melted regions were compared with the experimental results as plotted in Figures 8(a) and 8(b) respectively. As to the widths, the simulation results are in good agreement with the experimental results although the result of the laser condition D (where the spot diameter is 2.87 mm) had relatively larger error between the simulation and experiment. A similar tendency can be seen for the depths of the melted region where the error for the laser condition D is too large to be ignored. One of the reasons for the large error in the laser condition D is because the latent heat for the evaporation is not considered in the simulations. Assuming that the boiling temperature is 3000 °C, the volume of the evaporated particles, whose maximum temperatures are over the boiling temperature, are plotted in Figure 8(c). The evaporated volume is larger when the spot diameter is larger, and consequently the error between simulation and experiment also becomes higher. However, when the effect of the evaporation is not significant, the dimensions of the melted region corresponds quite well with the experimental results. Considering the latent heat for the evaporation is one of our future works.

5 CONCLUSIONS

New formulations for the heat conduction problem based on the LSMPS method were presented in order to simulate the laser irradiation on a metal block. The proposed method can conserve the total thermal energy and then more accurate simulations with external heat sources can be conducted when compared with the standard LSMPS method. It was revealed that the LSMPS-like flux method provides inaccurate results with the overshooting and undershooting for the non-regular particle arrangement, while the MPS-like flux method gives more accurate results even for irregular and multi-resolution particle distributions. When applied to the laser irradiation onto metal parts, the temperatures and the dimensions of the melted area were able to be well evaluated and the validity of the proposed method was successfully confirmed.

REFERENCES

[1] Ayoola, W. A., Suder, W. J. and Williams, S. W. Parameters controlling weld bead profile in conduction laser welding. *Journal of Materials Processing Technology* (2017) **249**:522-530.

[2] Cho, J. and Na, S. Implementation of real-time multiple reflection and Fresnel absorption of laser beam in keyhole. *Journal of Physics D: Applied Physics* (2006) **39**.

[3] Gingold, R. A. and Monaghan, J. J. Smoothed particle hydrodynamics - Theory and application to non-spherical stars. *Monthly Notices of the Royal Astronomical Society* (1977) **181**:375-389.

[4] Koshizuka, S., Tamako, H. and Oka, Y. A particle method for incompressible viscous flow with fluid fragmentation. *Computational Fluid Dynamics Journal* (1995) **4**:29-46.

[5] Sikarudi, M. A. E. and Nikseresht, A. H. Neumann and Robin boundary conditions for heat conduction modeling using smoothed particle hydrodynamics. *Computer Physics Communications* (2016) **198**:1-11.

[6] Tamai, T. and Koshizuka, S. Least squares moving particle semi-implicit method. *Computational Particle Mechanics* (2014) **1**:277-305.

[7] Tanaka, M., Cardoso, R. and Bahai, H. Multi-resolution MPS method. *Journal of Computational Physics* (2018) **359**:106-136.